ADBA Computer Science
Cutting-Edge Scientific Solutions

e-ISSN: 3023-8544
RESEARCH ARTICLE
Vol.2 / No.2 / 2025 / pp.30-35
https://doi.org/10.69882/adba.cs.2025071

Chaos Annihilation-Based on Genetic Algorithms in a Non-smooth Air-gap Permanent Magnet Synchronous Motor Embedded in the Microcontroller

Isidore Komofor Ngongiah[*,1], **Rolande Tsapla Fotsa**[β,2], **Joseph Mvogo Ngono**[α,3], **Noel Nyang Kibanya**[γ,4], **Emile Godwe**[δ,5] **and Foutse Momo**[σ,6]

[*]Department of Mechanical, Petroleum and Gas Engineering, National Advanced School of Mines and Petroleum Industries, University of Maroua, P.O. Box 46, Maroua, Cameroon, [β]Department of Mechanical Engineering, College of Technology, University of Buea, P.O. BOX 63 Buea, Cameroon, [α]Applied Computing Laboratory, Faculty of Science, University of Douala, P.O. Box 2701, Douala, Cameroon, [γ]Department of Physics, Faculty of Science, University of Bamenda, P.O. Box 39 Bamenda, Cameroon, [δ]Department of Physics, Faculty of Science, University of Maroua, P.O. Box 814, Cameroon, [σ]Biomedical Engineering, Energy and Modeling Laboratory (BEEMo.Lab.), Higher Institute of Science and Technology (HIST), University of Mountains, P.O. Box 208, Bangangte, Cameroon.

ABSTRACT This paper is devoted to the dynamical probing, microcontroller execution, and chaos annihilation based on genetic algorithms (GAs) in a non-smooth air-gap permanent magnet synchronous motor (NSAGPMSM) without external disturbances. The numerical simulations of NSAGPMSM in the absence of external disturbances reveal the existence of two different shapes of chaotic characteristics, reverse period doubling and periodic characteristics. The dynamical characteristics are certified by the microcontroller execution of NSAGPMSM in the absence of external disturbances. By optimizing the parameters of NSAGPMSM in the absence of external disturbances, thanks to the convergence of the objective function and its convergence rate, it is proven that GAs is effective in optimizing system parameters, leading to annihilation of chaos in the system to one of its three steady states.

KEYWORDS
Non-smooth air-gap
Permanent magnet synchronous motor
Microcontroller execution
Annihilation of chaos
Genetic algorithms

INTRODUCTION

The introduction of high-performance permanent magnets, such as rare-earth magnets, has led to the development of a new generation of synchronous machines (Kiener *et al.* 1984; Pouillange 1987; Song *et al.* 2015). Due to their superior properties, such as high efficiency, compact size, high torque-to-weight ratio, high power density, fault tolerance, and low maintenance, permanent magnet synchronous motors are widely used in many industrial applications, such as machine tools, industrial robots, air conditioners, and packaging machines (Ananthamoorthy and Baskaran 2015; Chan and Chau 1997; Do *et al.* 2014a). However, these uses are not without challenges, particularly in the face of growing energy, industrial, and automotive concerns. Permanent magnet synchronous motors with non-smooth air gaps may exhibit instability during operation and may be subject to physical phenomena, such as chaos, which can lead to a complete collapse of the drive system (Machkour *et al.* 2022; Liao *et al.* 2017). These disturbances can be caused by mechanical vibrations (rotor imbalance), abrupt variations in the applied load, etc. To overcome these challenges, it is essential to develop innovative control strategies that take the performance of NSAGPMSM into account.

The high performance of permanent magnet synchronous motors depends on the absence of chaos (Iqbal and Singh 2019; Takougang Kingni *et al.* 2020; Tsapla Fotsa *et al.* 2025), without considering the impact of variations in the saliency ratio through the quadrature inductance. It should be noted that while variations in quadrature inductance are not always beneficial due to the potential for chaotic behavior, they can lead to an increase in the amplitude of angular velocity. However, it is important to note that in permanent magnet synchronous motors, the direct and

Manuscript received: 12 May 2025,
Revised: 16 July 2025,
Accepted: 16 July 2025.

[1]ngongiahisidore@gmail.com (**Corresponding author**)
[2]rtsapla@yahoo.com
[3] jmvogo@univ-douala.cm
[4]nyangnoelkibanya@gmail.com
[5]willgod7@yahoo.com
[6]mfoutse@yahoo.fr

quadrature inductances must be different (Yamdjeu *et al.* 2024, 2025).

To eliminate chaotic behaviors in permanent magnet synchronous motors, researchers have employed various control methods, such as control using Lyapunov's principle for global asymptotic stability (Kemnang Tsafack *et al.* 2020; Natiq *et al.* 2022; Do *et al.* 2014b), simple adaptive sliding mode control (Kemnang Tsafack *et al.* 2020; Maeng and Choi 2013), fuzzy adaptive control schemes (Luo 2014), passive control schemes (Wang *et al.* 2005), model predictive control, feedback control schemes (Du-Qu and Xiao-Shu 2008), dithering signal control schemes (Tung and Chen 1993; Wei and Wang 2013), and chaos control based on GAs to optimize the performance of NSAGPMSM with temperature through the objective function value (Yamdjeu *et al.* 2025; Cvetkovski and Petkovska 2016).The authors of (Yamdjeu *et al.* 2024) studied the dynamics, microcontroller implementation, and control approach in NSAGPMSM without external disturbances.

The NSAGPMSM without external disturbances displayed bistable chaos, periodic spikes, chaotic spikes, coexistence of periodic and chaotic characteristics, and a period-doubling route to monostable chaos. Two single controllers were used to bring chaos back to stable operation, with the second single controller being more effective due to its ability to meet selection criteria such as settling time and peak overshoot. Chaos annihilation based on GAs in NSAGPMSM without external disturbances embedded in the microcontroller is investigated in this paper.

The choice of the latter method is inspired by natural evolution, as GAs use techniques such as inheritance, mutation, selection, and crossover to generate solutions to optimization problems. Its versatility makes it a powerful tool for global optimization and the analysis of large data sets (Markku *et al.* 2007; Tian *et al.* 2019). Many researchers have focused on using GAs to reduce harmful vibrations or eliminate noise in permanent magnet synchronous motors (Pinto *et al.* 2024; Yi and Hsu 2003; Randi *et al.* 2013). This paper is organized into an introduction, two sections, and the conclusion: Section two presents the dynamical probing and microcontroller execution in NSAGPMSM without external disturbances. Section three brings out the chaos annihilation in NSAGPMSM without external disturbances based on GAs. The conclusion highlights a summary of the paper.

DYNAMICAL PROBING AND MICROCONTROLLER EXECUTION IN NSAGPMSM WITHOUT EXTERNAL DISTURBANCES

The PMSM is presented in Fig. 1.

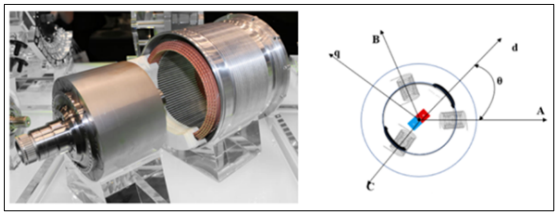

Figure 1 Permanent Magnet Synchronous Motors (PMSM) and its space representation (Grellet and Clerc 1997; Caron and Hautier 1995).

The PMSM is presented in Fig. 1. Phase transformation is a key technique in designing and controlling PMSM, converting a three-axis reference frame to a two-axis frame to simplify the motor's differential equations (Grellet and Clerc 1997). The machine electrical equations in matrix form is given by (Caron and Hautier 1995):

$$[V_{Sabc}] = [R][I_{Sabc}] + \frac{d}{dt}[\psi_{Sabc}], \tag{1}$$

The stator voltage V_{Sabc} is represented as a resistive term R multiplied by the axes current components I_{Sabc} and a flux variation term ψ_{Sabc}.

The magnetic equations defined by the stator flux equations can be expressed in matrix form as follows:

$$[\psi_{Sabc}] = [L][I_{Sabc}] + [\psi_{rabc}]. \tag{2}$$

The stator flux includes the self-flux and the flux generated by the magnets. The fluxes ψ_{rabc} are the rotor fluxes as seen by the stator windings given by:

$$\psi_{rabc} = \psi_m \begin{pmatrix} \cos\theta \\ \cos(\theta - 2\pi/3) \\ \cos(\theta - 4\pi/3) \end{pmatrix}, \tag{3}$$

where ψ_m is the constant magnet flux located along the direct axis of the (d-q) frame. The mechanical equation is given by:

$$C_{em} - C_r = J\frac{d\Omega_r}{d\tau} + f_v\Omega_r, \tag{4}$$

where C_{em} is the electromagnetic torque, C_r is the load torque, $\frac{d\Omega_r}{d\tau}$ is the angular acceleration, and f_v is the viscous friction. The electromagnetic torque is produced by the interaction between the poles formed by the magnets on the rotor and the poles generated by the magnetomotive forces in the air gap due to the stator currents given by:

$$C_{em} = \frac{3P}{2}(\psi_r I_q + (L_d - L_q)I_d I_q), \tag{5}$$

where the coefficient $3P/2$ denote the pole-pairs. Thanks to the Phase transformation and some mathematical manipulations, the set of equations describing the NSAGPMSM are given by:

$$L_d\frac{dI_d}{d\tau} = \mu_d - RI_d + \Omega_r L_q I_q, \tag{6a}$$

$$L_q\frac{dI_q}{d\tau} = \mu_q - RI_q - \Omega_r(L_d I_d - \psi_m), \tag{6b}$$

$$J\frac{d\Omega_r}{d\tau} = \frac{3P}{2}(\psi_r I_q + (L_d - L_q)I_d I_q) - C - f_v\Omega_r. \tag{6c}$$

With the following transformations: $\mu_d = \mu_q = C = 0$, $\tau = \omega_c t$, $\omega_c = L_q/R$, $\eta_p = \frac{3P}{2}$, $\delta = \frac{L_q}{L_d}$, $\epsilon = \epsilon_0(1-\delta)$, $\epsilon_0 = \frac{\omega_c^2 k^2 L_q}{J}$, $k = \frac{f_v}{\omega_c\eta_p\psi_r}$, $\sigma = \frac{f_v\omega_c}{J}$, $\gamma = \frac{\eta_p\psi_r}{kL_q}$, $I_d = \frac{k\delta}{\eta_p}i_d$, $I_q = ki_q$, and $\Omega_r = \frac{1}{\omega_c}\omega$, the corresponding system depicting the NSAGPMSM without external disturbances are [12, 31, 32]:

$$\frac{di_d}{dt} = -\delta i_d + \eta_p i_q\omega, \tag{7a}$$

$$\frac{di_q}{dt} = -i_q - i_d\omega + \gamma\omega, \tag{7b}$$

$$\frac{d\omega}{dt} = \sigma(i_q - \omega) + \epsilon i_d i_q, \tag{7c}$$

with the currents in the q- and d-coordinates defined respectively by i_q, i_d, the rotor's mechanical speed given by ω and $\delta, \eta, \gamma, \sigma, \epsilon$ the constant parameters. The local maxima of i_d and the corresponding greatest Lyapunov exponent (GLE) versus σ are depicted in Fig. 2.

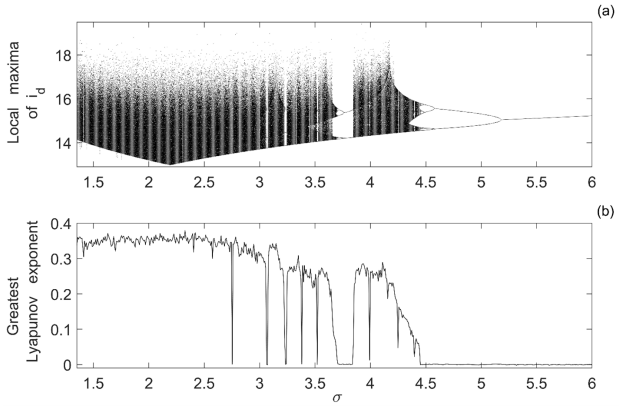

Figure 2 (a) Local maxima of i_d and associated GLE (b) versus σ for $\epsilon = 0.41$, $\gamma = 13.27$, $\eta_p = 1.0$ and $\delta = 0.2$.

Figure 2(a) displays chaotic region with windows of periodic characteristics, reverse period doubling, and limit cycle. The GLE plot in Fig. 2(b) confirms the dynamical characteristics encountered in Fig. 2(a). The chaotic characteristics encountered in Fig. 2 are depicted in Fig. 3.

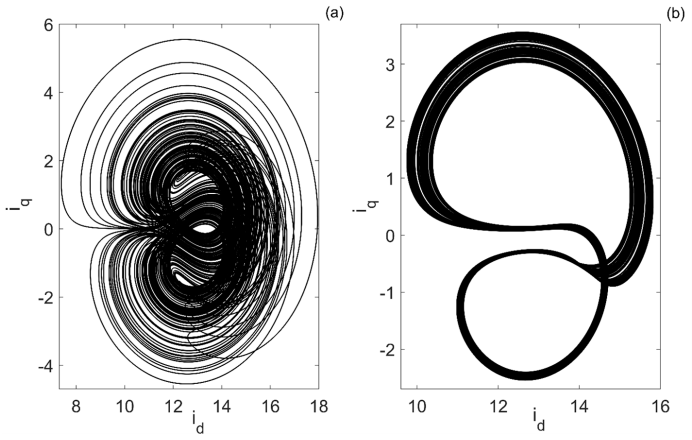

Figure 3 Phase plane trajectories in the plane (i_d, i_q) for given values of σ: (a) $\sigma = 1.4$ and (b) $\sigma = 4.44$. The other parameters are $\epsilon = 0.41$, $\gamma = 13.27$, $\eta = 1.0$, $\delta = 0.2$ and $(i_d(0), i_q(0), \omega(0)) = (0.01, 0.01, 0.01)$.

Two different shapes of chaotic characteristics are shown in Fig. 3. The shapes of chaotic attractors of Fig. 3 are different from the ones found in (Yamdjeu *et al.* 2024).

Figure 4 shows the microcontroller execution setup of NSAGPMSM described by system (7).

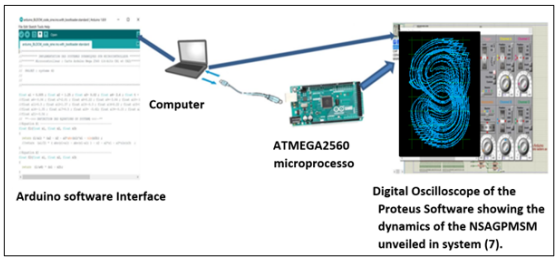

Figure 4 Microcontroller execution setup of NSAGPMSM without external disturbances described by system (7).

Figure 4 depicts the microcontroller experimental setup comprised of the ATmega2560 microcontroller, featuring an 8-bit AVR architecture and operating at a clock speed of 16 MHz. It includes 256 KB of flash memory, with 8 KB allocated for the bootloader, along with 8 KB of static random-access memory and 4 KB of electrically erasable programmable read-only memory. The microcontroller offers 54 digital input/output pins, 16 analog input pins, and supports various communication protocols, making it ideal for complex projects. The input and output of the Arduino Mega ATMEGA2560 are respectively connected to the computer and an oscilloscope of clock frequency 16 MHz through a R-2R resistor network. The program of system (7) describing the NSAGPMSM without external disturbances solved through the 4^{th}-order Runge-Kutta scheme using the software Arduino compiler is then inserted in the Arduino Mega microcontroller, which delivers its output signal through the R-2R resistor network. The R-2R resistor network transforms the digital signals into an equivalent analog signal, which is employed to feed the oscilloscope of the Proteus software. The dynamical characteristics encountered in Fig. 3 are established in Fig. 5 from the microcontroller execution setup of Fig. 4.

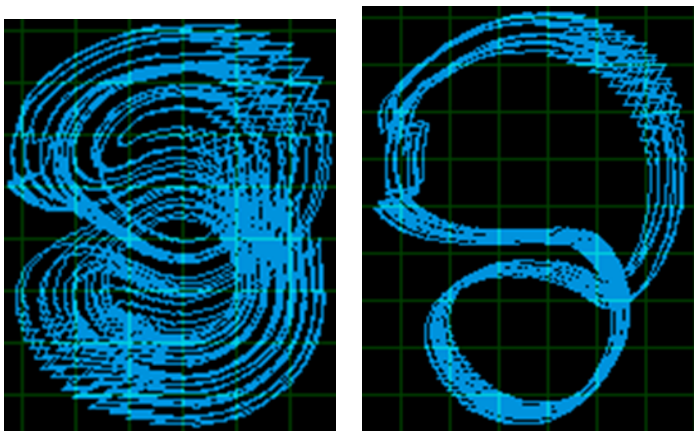

Figure 5 Microcontroller results of NSAGPMSM without external disturbances described by system (7): (a, b) have the same parameters as those in Figs. 3 (a, b).

The experimental phase plane projections of Fig. 5 found from Fig. 4 confirm the phase plane projections of Fig. 3 obtained numerically.

CHAOS ANNIHILATION IN NSAGPMSM WITHOUT EXTERNAL DISTURBANCES BASED ON GAS

The GAs enhances the robustness of chaotic systems by enabling global and multi-objective optimization across various engineering fields, such as mechanical, power, chemical, robotics, and aerospace engineering. They effectively control chaotic behaviors, improving safety and performance in real-world applications like ship roll and hybrid piecewise-smooth systems. Inspired by natural selection, genetic algorithms utilize concepts like fitness functions, mutation, and selection to iteratively create new populations, successfully addressing chaos in both discrete and continuous systems without needing complex derivations or integrations (Venkatesh *et al.* 2025). The chaotic characteristics encountered in NSAGPMSM without external disturbances are controlled based on GAs. The objective function is given by:

$$\text{fitness} = \frac{1}{n}\sum_{i=1}^{n} |X_i - E_i|, \tag{8}$$

where $X_i = (i_q, i_d, \omega)^t$ and E_i is the equilibrium point. For $\epsilon = 0.41$, $\eta_p = 1.0$, $\sigma = 1.4$, $\delta = 0.2$, and $\gamma = 13.27$, Based on (Yamdjeu *et al.* 2024), the following three steady states are obtained for $\epsilon = 0.41$, $\eta_p = 1.0$, $\sigma = 1.4$, $\delta = 0.2$ and $\gamma = 13.27$: $E_1 = (0.0, 0.0, 0.0)^t$, $E_2 = (13.06276867, 0.7358009139, 3.550625834)^t$ and $E_3 = (13.06276867, -0.7358009139, -3.550625834)^t$. For a more stable convergence and to be adaptable to the system, the limits for each parameter $\sigma, \delta, \eta_p, \epsilon, \gamma$ are defined with the initial states $(i_q(0) = 0.01, i_d(0) = 0.01, \omega(0) = 0.01)$ after adjusting the parameters of the GAs. To suppress the chaos encountered in NSAGPMSM described by system (7) to the equilibrium point E_1, the optimized parameters of system (7) found are given in Table 1.

Table 1 Optimized parameters of NSAGPMSM described by system (7) based on AGs to suppress the chaos to the equilibrium point E_1.

Parameter	Value
σ	-0.33552431
δ	3.96840578
η_p	2.46271175
ϵ	-1.77251272
γ	8.06415182

Using the optimized parameters of Table 1, the objective function, change rate, error states, optimized phase diagram, and time evolutions of state variables are simulated and exposed in Fig. 6.

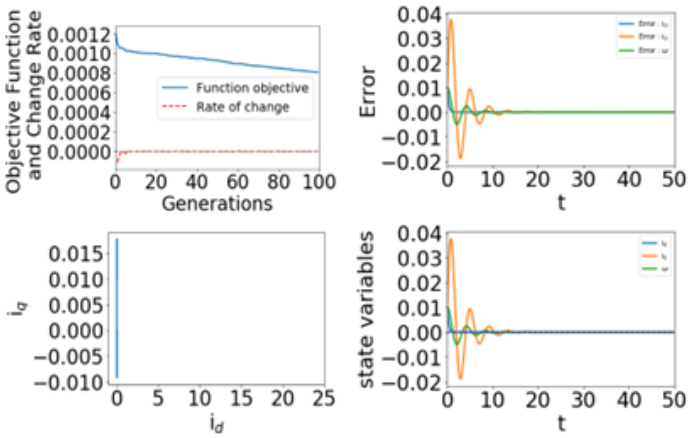

Figure 6 (a) Objective function and convergence rate versus the iteration, (b) time evolution of the error state variables, (c) optimized phase diagram in the (i_d, i_q) plane, and (d) optimized state variables.

To suppress the chaos encountered in system (7) to the equilibrium point E_2, the optimized parameters of system (7) found are given in Table 2.

Table 2 Optimized parameters of NSAGPMSM described by system (7) based on AGs to suppress the chaos to the equilibrium point E_2.

Parameter	Value
σ	0.79055438
δ	0.77378635
η_p	3.49183549
ϵ	0.20809594
γ	13.23148673

Using the optimized parameters of Table 2, the objective function, change rate, error states, optimized phase diagram, and time evolutions of state variables are simulated and exposed in Fig. 7.

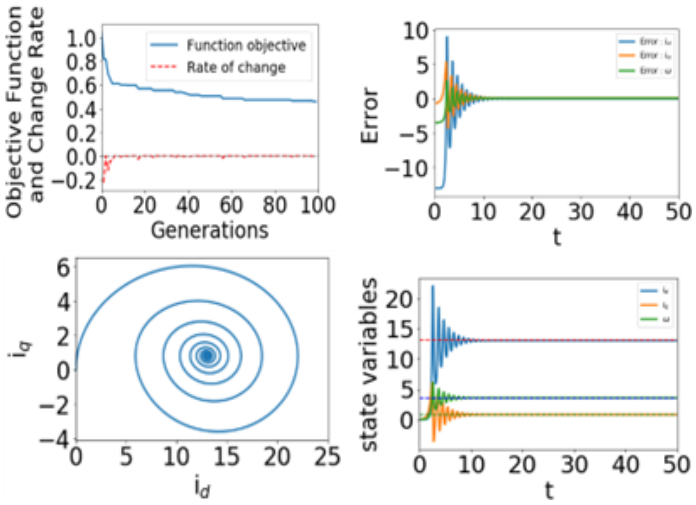

Figure 7 (a) Objective function and convergence rate versus the iteration, (b) time evolution of the error state variables, (c) optimized phase diagram in the (i_d, i_q) plane, and (d) optimized state variables.

To suppress the chaos encountered in NSAGPMSM described by system (7) to the equilibrium point E_0, the optimized parameters of system (7) found are given in Table 3.

Table 3 Optimized parameters of NSAGPMSM described by system (7) based on AGs to suppress the chaos to the equilibrium point E_0.

Parameter	Value
σ	0.921774470
δ	0.57436885
η_p	2.85432314
ϵ	0.2727070
γ	13.26536079

Using the optimized parameters of Table 3, the objective function, change rate, error states, optimized phase diagram, and time evolutions of state variables are simulated and exposed in Fig. 8.

The objective functions stabilize after decreasing with the number of iterations, and the convergence rates tend towards zero,

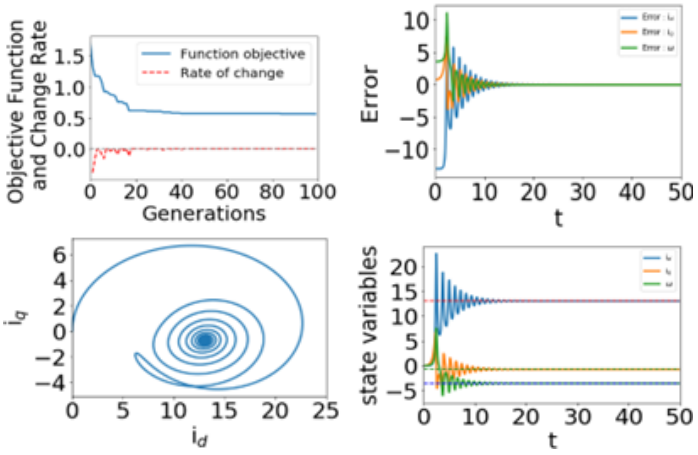

Figure 8 (a) Objective function and convergence rate versus the iteration, (b) time evolution of the error state variables, (c) optimized phase diagram in the (i_d, i_q) plane, and (d) optimized state variables.

which provides information on the efficiency and speed with which the GAs reach an optimal solution as shown in Figs. 6(a), 7(a), and 8(a). The time evolutions of the errors of the state variables in Figures 6(b), 7(b), and 8(b) converge to zero. GAs is effective to suppress chaos found in NSAGPMSM described by system (7) to the steady state E_i, as illustrated in Figs. 6(c, d), 7(c, d), and 8(c, d).

CONCLUSION

The paper was devoted to the numerical, microcontroller implementation, and chaos annihilation methods in a non-smooth air-gap permanent magnet synchronous motor (NSAGPMSM) without external disturbances. Two different shapes of chaotic characteristics, reverse period doubling and periodic characteristics, were encountered in NSAGPMSM without external disturbances. These dynamical characteristics found numerically in NSAGPMSM without external disturbances were confirmed by the microcontroller execution of NSAGPMSM without external disturbances. By optimizing the parameters of NSAGPMSM without external disturbances based on genetic algorithms, the chaotic characteristics encountered in NSAGPMSM without external disturbances converged to one of its three steady states. In future considerations, additional control schemes and optimization methods such as Particle Swarm Optimization (PSO), Differential Evolution (DE), and classical Proportional-Integral-Derivative (PID) tuning will be utilized to mitigate complex behaviors in the NSAGPMSM. A comparison will be made to highlight the similarities and differences with the approaches discussed in this paper.

Ethical standard

The authors have no relevant financial or non-financial interests to disclose.

Availability of data and material

Not applicable.

Conflicts of interest

The authors declare that there is no conflict of interest regarding the publication of this paper.

LITERATURE CITED

Ananthamoorthy, N. P. and K. Baskaran, 2015 High performance hybrid fuzzy pid controller for permanent magnet synchronous motor drive with minimum rule base. Journal of Vibration and Control **21**: 181.

Caron, J. P. and J. P. Hautier, 1995 *Modélisation et commande de la machine asynchrone*, volume 10. Technip, Paris.

Chan, C. C. and K. T. Chau, 1997 An overview of power electronics in electric vehicles. IEEE Transactions on Industrial Electronics **44**: 3.

Cvetkovski, G. and L. Petkovska, 2016 Multi-objective optimal design of permanent magnet synchronous motor. In *IEEE International Power Electronics and Motion Control Conference*, p. 605.

Do, T. D., E. K. Kim, J. W. Jung, V. Q. Leu, and H. H. Choi, 2014a Adaptive pid speed control design for permanent magnet synchronous motor drives. IEEE Transactions on Power Electronics **30**: 900.

Do, T. D., E. K. Kim, J. W. Jung, V. Q. Leu, and H. H. Choi, 2014b Adaptive pid speed control design for permanent magnet synchronous motor drives. IEEE Transactions on Power Electronics **30**: 900.

Du-Qu, W. and L. Xiao-Shu, 2008 Passive adaptive control of chaos in synchronous reluctance motor. Chinese Physics **17**: 92.

Grellet, G. and G. Clerc, 1997 *Electric actuators*. Eyrolles editions.

Iqbal, A. and G. K. Singh, 2019 Chaos control of permanent magnet synchronous motor using simple controllers. Transactions of the Institute of Measurement and Control **41**: 2353.

Kemnang Tsafack, A. S., R. Kengne, J. R. M. Pone, S. Takougang Kingni, A. Cheukem, *et al.*, 2020 Spiking oscillations and multistability in nonsmooth-air-gap brushless direct current motor: Analysis, circuit validation and chaos control. International Transactions on Electrical Energy Systems **12**.

Kiener, A., P. Brissonneau, L. Brugel, and J. P. Yonnet, 1984 Conception des moteurs à aimants. Revue Générale de l'Électricité pp. 313–318.

Liao, X., F. Zhang, and C. Mu, 2017 Dynamical analysis of the permanent synchronous motor chaotic system. Advances in Difference Equations **2017**: 2.

Luo, S., 2014 Adaptive fuzzy dynamic surface control for the chaotic permanent magnet synchronous motor using nussbaum gain. Chaos **24**: 2.

Machkour, N., C. Volos, K. Kemih, H. Takhi, L. Moysis, *et al.*, 2022 Predictive control and synchronization of uncertain perturbed chaotic permanent-magnet synchronous generator and its microcontroller implementation. The European Physical Journal Special Topics **231**.

Maeng, G. and H. Choi, 2013 Adaptive sliding mode control of a chaotic nonsmooth-air-gap permanent magnet synchronous motor with uncertainties. Nonlinear Dynamics **74**: 572.

Markku, N., J. Hilla, P. Salminen, and J. Pyrhönen, 2007 Guidelines for designing concentrated winding fractional slot permanent magnet machines. In *International Conference on Power Engineering, Energy and Electrical Drives*, p. 191.

Natiq, H., J. Metsebo, A. S. Kemnang Tsafack, B. Ramakrishnan, A. C. Chamgou, *et al.*, 2022 Synchronous reluctance motor: Dynamical analysis, chaos suppression, and electronic implementation. Journal of Complexity pp. 1–7.

Pinto, T., G. Cong, T. Nguyen Vu, and Q. Vuong, 2024 Optimization design of surface-mounted permanent magnet synchronous motors using genetic algorithms. EAI Endorsed Transactions on Energy **11**: e5.

Pouillange, J. P., 1987 Les machines synchrones à aimants perma-

nents. Revue Génále de l'Électricité pp. 17–21.
Randi, S., R. Benlamine, F. Dubas, and C. Espanet, 2013 Design by optimization of an axial flux permanent-magnet synchronous motor using genetic algorithms. In *International Conference on Electrical Machines and Systems*, volume 13.
Song, J. H., Y. Cho, K. B. Lee, and Y. I. Lee, 2015 Torque-ripple minimization and fast dynamic scheme for torque predictive control of permanent magnet synchronous motors. IEEE Transactions on Industrial Electronics **30**: 2182.
Takougang Kingni, S., A. C. Chamgou, A. Cheukem, A. S. K. Tsafack, and J. R. M. Pone, 2020 Permanent magnet synchronous motor: Chaos control using single controller, synchronization and circuit implementation. SN Applied Sciences **2**.
Tian, C., C. Wu, X. Huang, and P. Zhang, 2019 Multi-physical field optimization analysis of high-speed permanent magnet synchronous motor based on nsga-ii algorithm. In *22nd International Conference on Electrical Machines and Systems*, volume 6, p. 5.
Tsapla Fotsa, R., P. K. Koubeu Papemsi, G. P. Ayemtsa Kuete, J. R. Mboupda Pone, S. R. Dzonde Naoussi, *et al.*, 2025 Title of Forthcoming Article. Chaos and Fractals **2**: 14–19, Bibliographic details are for a future publication.
Tung, P. C. and S. C. Chen, 1993 Experimental and analytical studies of the sinusoidal dither signal in a dc motor system. Dynamics and Control **3**: 54.
Venkatesh, J., A. T. Kouanou, I. K. Ngongiah, D. C. Sekhar, and S. T. Kingni, 2025 Dynamical probing and suppressing chaos using genetic algorithms in a josephson junction model with quadratic damping embedded in the microcontroller implementation. Journal of Vibration Engineering & Technologies **13**: 8–24.
Wang, J. J., D. L. Qi, and G. Z. Zhao, 2005 Multi-shelled hollow micro-/nanostructures. Journal of Zhejiang University Science **6**: 729.
Wei, Q. and X. y. Wang, 2013 Chaos controlling of permanent magnet synchronous motor base on dither signal. Journal of Vibration and Control **19**: 2541.
Yamdjeu, G., B. Sriram, S. Takougang Kingni, D. Chandra Sekhar, and A. Mohamadou, 2025 Non-smooth-air-gap permanent magnet synchronous motor under the effect of temperature embedded in the microcontroller: Dynamical appraisal and chaos suppression employing genetic algorithms. Journal of Vibration Engineering & Technologies **13**: 170.
Yamdjeu, G., B. Sriram, S. Takougang Kingni, K. Rajagopal, and A. Mohamadou, 2024 Analysis microcontroller implementation and chaos control of non-smooth air-gap permanent magnet synchronous motor. Pramana - Journal of Physics **98**: 126.
Yi, L. and A. Hsu, 2003 Efficiency optimization of brushless permanent magnet motors using penalty genetic algorithms. In *IEEE International Electric Machines and Drives Conference*, volume 1, p. 365.

How to cite this article: Ngongiah, I. K., Fotsa, R. T., Ngono, J. M., Kibanya, N. N., Godwe, E., and Momo, F. Chaos Annihilation-Based on Genetic Algorithms in a Non-smooth Air-gap Permanent Magnet Synchronous Motor Embedded in the Microcontroller. *ADBA Computer Science*, 2(2), 30-35, 2025.